Ferroelectrics, 379:191–198, 2009

ISSN: 0015-0193 print / 1563-5112 online
DOI: 10.1080/00150190902852240

Taylor & Francis
Taylor & Francis Group

The Effect of Oxygen Vacancies on the Atomic and Electronic Structure of Cubic ABO_3 Perovskite Bulk and the (001) Surface: *Ab initio* Calculations

Y. F. ZHUKOVSKII,[1,2,*] E. A. KOTOMIN,[1,2,3] S. PISKUNOV,[1,2,4] Y. A. MASTRIKOV,[1,3] AND D. E. ELLIS[2]

[1]Institute for Solid State Physics, University of Latvia, 8 Kengaraga Str., Riga LV-1063, Latvia
[2]Materials Research Center, Northwestern University, 2145 Sheridan Rd., Evanston IL, 60208, USA
[3]Max Planck Institute for Solid State Research, Heisenbergstr. 1, 70569 Stuttgart, Germany
[4]Lehrstuhl für Theoretische Chemie, Universität Duisburg-Essen, Universitätstr. 2, 45141 Essen, Germany

We employed the hybrid DFT-LCAO and GGA-PW approaches as implemented in the CRYSTAL and VASP codes, respectively, for large supercell calculations of neutral O vacancies with trapped electrons (known as F centers) in the bulk and on the (001) surface of three cubic perovskite crystals ($SrTiO_3$, $PbTiO_3$, and $PbZrO_3$). The local lattice relaxation, charge redistribution, and positions of defect energy levels within the band gap are compared for three perovskites under study. We demonstrate how the difference in chemical composition of host materials leads to quite different defect properties.

Keywords ABO_3 perovskites; low index surfaces; F-center; DFT calculations

Introduction

ABO_3–type ternary metal oxides (perovskites) comprise a rich family of crystalline structures: simple cubic (Fig.1a), tetragonal, orthorhombic, *etc.,* which correspond to the ferroelectric, antiferroelectric, and other phases with specific, technologically important properties. In spite of substantial efforts, the nature of defects in ABO_3 perovskites is still an open question [1]. One of the most common and important point defect in perovskites is an *oxygen vacancy* with trapped electrons, called the color *F center*. More precisely, these defects in partly covalent perovskites resemble the *E*' centers (Si dangling bonds) formed in several oxides and silicates, where each O ion is surrounded by only two nearest neighbor positively charged ions [2] rather than the traditional *F* centers in MgO-type ionic solids where two electrons are thus strongly localized by the Madelung field in the O vacancy. However, the analogy with *E*' centers is also incomplete since this should lead to the creation of Me−Me bonds and strong displacements

Received June 15, 2008.
*Corresponding author. E-mail: quantzh@latnet.lv

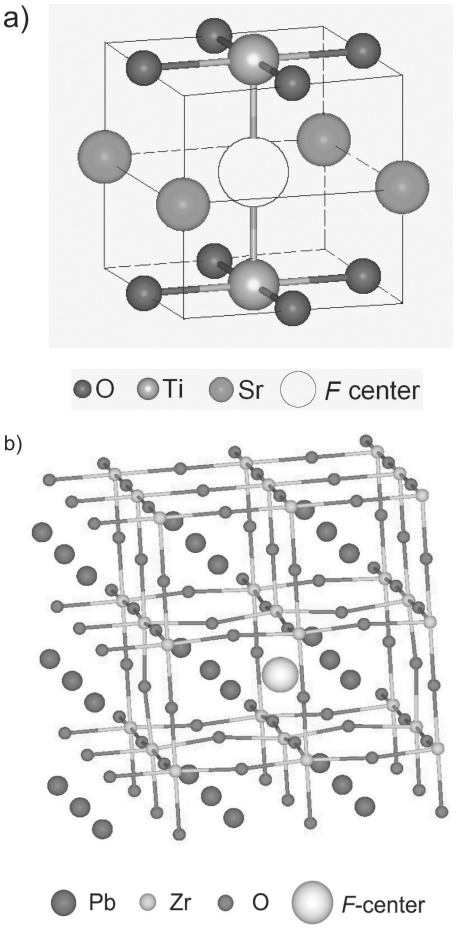

Figure 1. (a) Unit cell of defective cubic $SrTiO_3$, (b) $3 \times 3 \times 3$ supercell model of cubic $PbZrO_3$ perovskite with an O vacancy. (See Color Plate XVII)

of both Me ions towards each other. Thus, O vacancies in perovskites really cannot be attributed to earlier defined type of color centers; yet for simplicity we continue to call them *F* centers. Detailed analysis of previous calculations performed on the *F* centers in binary and ternary metal oxides is summarized in several books and review articles [1–11].

In this paper, we present a *comparative study* of the *F* centers in cubic phases of three key perovskites: $SrTiO_3$ (or STO, widely used as a substrate for growth of high-T_c superconductors), $PbTiO_3$ (PTO, actuators and sonar devices) and $PbZrO_3$ (PZO, charge storage and diagnostic material for radiation environment), both bulk and (001) surface. The cubic phase is stable in STO at room temperature; for both PTO and PZO it is a high- temperature phase. Since in this study we are interesting mostly in analyzing how variation in A and B cations affect the properties of pure and defective perovskite materials, we consider here the high-symmetry cubic phase. One of the main characteristics of a defective crystal is position of its defect levels with respect to the valence (conduction) band of the pure material which controls electron/hole localization and defect stability.

This means that any theoretical method used to describe a defective structure should reproduce reliably the band gap of the crystal (~3 eV in perovskites). As is well known [11], classical LDA and GGA functionals within DFT underestimate the band gap (up to a factor of two for perovskites) whereas the Hartree-Fock scheme drastically overestimates it. On the other hand, our experience obtained on *ab initio* simulations on ABO_3 perovskites [12, 13] argues that the *hybrid functionals* (B3LYP, B3PW) are the most reliable techniques able to reproduce band gaps of wide-gap materials with high accuracy. These functionals are incorporated into the *CRYSTAL* code employed in this study (and used successfully for different material modeling [1-4]). The current version of the *VASP* code does not yet contain hybrid functionals [14], thus, we apply for our calculations the exchange-correlation functional based on the Generalized Gradient Approximation (GGA).

Method

Periodic structure calculations of perfect and defective perovskites (Fig. 1) have been performed using the *CRYSTAL* code [15] with the hybrid B3PW exchange correlation functional [16] which consists of the mixture of the non-local exact Fock exchange and GGA exchange functionals using Becke's three parameter method. CRYSTAL employs atom-centered Gaussian-type functions as basis sets (BSs). The BS for Ti, Pb and O were taken from Ref. [13], while the BS for Zr from Ref.[15]. The inner core electrons of Ti, Pb, Zr atoms are described by the Hay-Wadt effective core pseudopotentials [17]. When modeling defects, a simple cubic (high-temperature) unit cell containing one formula unit (5 atoms) was extended to a $3 \times 3 \times 3$ supercell [9, 10]. (Our calculations performed on the electronic structure of bulk PZO for *both* cubic and orthorhombic phases yield only negligible difference in defect formation energy when oxygen vacancy is considered.) The effect of the supercell size was also recently analyzed in detail for the F centers in STO [19]). The distance between periodically repeated defects is ~12.5 Å when a $3 \times 3 \times 3$ supercell is used.

To simulate the F center, a *ghost* basis set was centered on an O vacancy [15]. This allows us to reproduce correctly the electronic density redistribution caused by the defect. In surface F center calculations we employed $2\sqrt{2} \times 2\sqrt{2}$ and 3×3 slab supercells containing seven planes (stacked planes of AO and BO_2 stoichiometry). The equilibrium geometry was obtained using the analytical optimization approach as implemented in the *CRYSTAL* code. To get equilibrium geometry of crystalline structure around O vacancies in cubic ABO_3 perovskites, the atomic sites from eight coordination spheres nearest to the F center have been relaxed, keeping their spherical symmetry.

The reciprocal space integration was performed by a sampling the Brillouin zone with $8\times8\times8$ and $4\times4\times4$ Pack-Monkhorst and Gilat k-point meshes [20, 21] for defective bulk perovskites and the defective (001) surface, respectively. To analyze the charge redistribution caused by the defects, the effective atomic charges were characterized using the static (Mulliken) population analysis. To study defect mobility, additional GGA-PW calculations were performed using the *VASP* code [22].

Bulk Properties

Perfect Perovskites

The optimized cubic lattice constants a_0 are very close to the experimental high-temperature values (Table 1) (notice that a_0 for PZO considerably exceeds that for the other two

Table 1

The Mulliken effective atomic charges q (in e), bond populations p (milli e), direct band gaps $\Delta\varepsilon_{gap}$ (eV) and lattice constants a_o (Å) calculated for three cubic bulk ABO_3 perovskites. Negative bond populations mean atomic repulsion. Experimental data are given in brackets

Property	$PbTiO_3$	$PbZrO_3$	$SrTiO_3$
q(A), e	1.34	1.30	1.87
q(B), e	2.33	2.07	2.35
q(O), e	−1.23	−1.12	−1.41
p(A-O), me	16	36	−10
p(B-O), me	98	100	88
p(O-O), me	−50	−20	−44
$\Delta\varepsilon_{gap}$, eV	2.87(3.40)	3.79 (3.70)	3.63 (3.75)
a_o, Å	3.93 (3.97)	4.18 (4.16)	3.91 (3.89)

pervoskites). A good agreement between experimental and theoretical values is observed also for the indirect band gaps. The effective Mulliken charges indicate a considerable covalency of the B-O chemical bonds. There is also a weak Pb-O covalent-bonding component in lead perovskites, unlike negligible Sr-O covalency in STO. The Mulliken charges show correspondingly also that the Sr is considerably more ionic than Pb.

Defective Perovkites

The different nature of a chemical bonding in Pb- and Sr- as well as Ti- and Zr-containing perovskites (the above mentioned partial Pb-O bond covalency *vs.* almost nominal ionic charge for Sr^{2+} as well as larger ionicity of Zr as compared to Ti atoms) results in a noticeable difference in the character of a lattice relaxation around point defects and other properties. Relative outward displacements of ions surrounding the F centers, compared to ideal crystal sites are 1 *vs.* 3% for the two nearest Zr and Ti ions in defective PZO and PTO perovskites, respectively; *i.e.* Zr is rather insensitive to the presence of an oxygen vacancy. However, the inward relaxation of the eight next-nearest oxygens around the F center is markedly larger in zirconate: cf. 10 *vs.* 2% for PZO and PTO, respectively. The same is true for relaxation of the next four neighboring Pb ions towards the defect: 12 *vs.* 5%. These two kinds of displacements reflect a trend to maintain the Pb-O bond covalency between the relaxed atoms. At the same time, behaviour of Sr is completely opposite to Pb; it is practically indifferent to the presence of O vacancy with outward displacement of 1%, although relaxation of B (Ti, Zr) and O atoms nearest to the F center in STO is closer to the relaxations in PTO than in PZO.

According to the Mulliken population analysis, the *O vacancy* traps 0.7 e, 0.9 e, and 1.2 e in PZO, PTO, and STO, respectively. Charge transfer towards two nearest Ti ions in PTO and STO is ∼0.25 e larger than to Zr ions in PZ, mainly due to higher covalency of the Ti-O bond as compared to Zr-O. Simultaneously, the O ionicity in STO is ∼0.2-0.3 e higher than those in PTO and PZ, due to partial covalency of the Pb-O bonds. This is well confirmed by a comparative analysis of the difference electron density, which clearly demonstrates an involvement of Pb, Zr and Ti ions in the defect-changed bond covalency with oxygens, whereas Sr ions are practically indifferent to defect-induced

Table 2

A comparative analysis of main bulk properties of defective $PbTiO_3$, $PbZrO_3$, and $SrTiO_3$ perovskites, calculated with the hybrid exchange-correlation functional. The $\Delta\varepsilon_{F-CB}$ is a distance from the conduction band bottom (CB), δ_F the defect band dispersion (eV), E^{form} the formation energy (eV).

Perovskite	Atoms of ABO_3 nearest to vacancy	Mulliken charge q, e		Parameters of defect level, eV		E^{form}, eV
		perfect crystal	defective crystal	$\Delta\varepsilon_{F-CB}$	δ_F	
$PbTiO_3$	F center[a]	–	0.85	0.96	0.21	7.82
	Ti	2.33	2.32			
	O	−1.23	−1.23			
	Pb	1.34	1.25			
$PbZrO_3$	F center[a]	–	0.68	1.71	0.14	7.25
	Zr	2.07	2.09			
	O	−1.12	−1.14			
	Pb	1.30	1.17			
$SrTiO_3$	F center[a]	–	1.21	0.69	0.25	8.74
	Ti	2.35	2.34			
	O	−1.41	−1.42			
	Sr	1.87	1.86			

[a] An excess of the electron density with respect to an empty vacancy.

changes [10]. The calculated band structure for the cubic PZO, PTO, and STO containing the F centers (Table 2 and Ref. [10]) also show differences between the F centers in these materials. The F center in PZO is a deep defect, with the donor level close to the middle of the gap, 1.7 eV below the bottom of conduction band (CB). The defect energy band caused by the interaction of periodically repeated defects has a small dispersion over the Brillouin zone (0.14 eV). In contrast, in PTO and STO perovskites, the defect level is much closer to the CB bottom, being characterized by a larger dispersion. As to the defect formation energy, it is noticeably larger for STO than for PZO and PTO (see Table 2).

The migration energy for the F center in the STO bulk has been calculated using the *VASP* code. The lattice was relaxed at each step along the migration path of O ion. The obtained values of 0.4–0.5 eV for the vacancy jumps between the nearest O sites along the (110) direction are in reasonable agreement with the experimental data [19]. It is not easy to check these results using the *CRYSTAL* code since oxygen vacancy in the ground state has only one ghost function centered at the vacancy site whereas at the saddle point we have two semi-vacancies which need use of two ghost functions, that is, these two calculations have two different basis sets.

Surface Properties

Numerous calculated properties of pure PTO,PZO and STO(001)surfaces were analyzed by us recently [23, 24]. The main properties of the surface F center on ABO_3(001) perovskites considered here are summarized in Table 3. The formation energies E^{form} of the F centers

Table 3
Calculated parameters of surface F centers (Notation is the same as in Table 2).

	Parameters of defect level, eV			
Perovskite	$\Delta\varepsilon_{F\text{-}CB}$	δ_F	Mulliken charge q_F^a, e	E^{form}, eV
$PbTiO_3$	0.71 [b]	0.08 [b]	0.41[b]	5.99[b]
$PbZrO_3$	2.44[c]	0.06[c]	0.30[c]	5.82[c]
	2.58[b]	0.03[b]	0.31[b]	7.00[b]
$SrTiO_3$	0.25 [b]	0.14 [b]	0.22 [b]	6.22 [b]

[a)]Excess of the electron density with respect to an empty vacancy;
[b)]3 × 3 BO_2-terminated surface supercell
[c)]$2\sqrt{2} \times 2\sqrt{2}$ BO_2-terminated surface supercell.

on the ABO_3(001) surface (Table 3) are considerably reduced as compared to those in bulk (Table 2), which stimulates their effective segregation from subsurface layers. The distance of the defect level to the conduction band (CB) bottom (which is close to the ionization energies) on PTO and STO (001) surfaces are substantially smaller than in the bulk; *i.e.*, the defect level becomes even more shallow on the surface. However, this is not the case for the PZO(001) surface where the F center is found to be a deep defect in both bulk (Table 2) and on the (001) surface (Table 3). In fact, the F-defect level on the PZO surface lies in the middle of the band gap, between the top of the valence band and bottom of CB (for both $2\sqrt{2}\times2\sqrt{2}$ and 3×3 surface supercells considered recently [24]). As compared to the bulk case, the electron density localized in the (001) surface oxygen vacancy (Table 3) is reduced; *e.g.*, from 0.7 e down to 0.3 e in PZO, due to the larger electron density delocalization over the two nearest B ions.

The surface F center migration energies calculated using the *VASP* code for the STO(001) defective surface have been found to be 0.19 eV and 0.11 eV for the $2\sqrt{2}\times2\sqrt{2}$ and $3\sqrt{2}\times3\sqrt{2}$ surface supercells, respectively; *i.e.*, by a factor of 2-3 smaller than in the bulk [19]. Despite known shortcomings of the DFT calculations for shallow defects, we believe that this qualitative conclusion is correct.

Conclusions

The hybrid exchange-correlation functional calculations combined with the supercell model permit a detailed study of point defects (*e.g.*, O vacancies) in advanced perovskite materials, including the ionization energies of shallow donors which control material conductivity and defect (and thus radiation-) stability. Thus, the results obtained here for the O vacancies in three types of defective cubic ABO_3 perovskites show a strong defect property dependence on the chemical nature of A and B atoms. The same F centers are shown to be deep defects in $PbZrO_3$ and shallow in $PbTiO_3$ and $SrTiO_3$. This is true also for the surface O vacancies: these produce shallow defects upon the STO and PTO (001) surfaces but deep defects on PZO (001) surface.

Acknowledgments

This study was supported by the Latvian National Program on Materials Science as well as the MRSEC Program of the National Science Foundation (DMR- 0520513) at the

Materials Research Center of Northwestern University (NU), Evanston (USA). SP gratefully acknowledges also funding from the European Social Fund (ESF). Authors kindly thank J. Maier, A. Sternberg, V. Alexandrov, R.A. Evarestov, E. Heifets, E. Spohr, and F. Illas for many stimulating discussions.

References

1. H.-J. Donnerberg, Atomic simulations of Electro-Optical and Magneto-Optical Materials (Springer Tracts in Modern Physics, Vol. 151; Berlin: Springer, 1999).
2. A. L. Shluger, A. S. Foster, J. L. Gavartin, and P. V. Sushko, Models of defects in wide-gap oxides: Perspective and challenges. In: *Nano and Giga Challenges in Microelectronics* (Eds. J. Greer and A. Korkin; North Holland: Elsevier, 2003) 151–222.
3. Quantum-Mechanical *Ab initio* Calculations of the Properties of Crystalline Materials (Ed. C. Pisani; Springer Lecture Notes in Chemistry, Vol. 67; Berlin: Springer, 1996).
4. E. A. Kotomin and A. I. Popov, Radiation-induced point defects in simple oxides. *Nucl. Instr. Meth. Phys. Res. B* **141**, 1–15 (1998).
5. M. V. Ganduglia-Pirovano, A. Hoffmann, and J. Sauer, Oxygen vacancies in transition metal and rare earth oxides: Current state of understanding and remaining challenges. *Surf. Sci. Reports* **62**, 219–270 (2007).
6. P. A. Cox, Transition Metal Oxides: an Introduction to their Electronic Structure and Properties (Oxford, UK: Clarendon Press, 1995).
7. W. Hayes and A. M. Stoneham, Defects and Defect Processes in Nonmetallic Solids (2nd Ed., Mineola, NY: Dover Publications Inc., 2004).
8. D. E. Ellis and O. Warschkow, Evolution of classical/quantum methodologies: applications to oxide surfaces and interfaces. *Coord. Chem. Rev.* **238/239**, 31–53 (2003).
9. R. A. Evarestov, Quantum Chemistry of Solids. The LCAO First Principles Treatment of Crystals (Springer Series in Solid State Sciences, Vol. 153; Heidelberg: Springer, 2007).
10. Yu. F. Zhukovskii, E. A. Kotomin, R. A. Evarestov, and D. E. Ellis, Periodic models in quantum chemical simulations of *F* centers in crystalline metal oxides. *Int. J. Quant. Chem.* **107**, 2956–2985 (2007).
11. R. Dovesi, R. Orlando, C. Roetti, C. Pisani, and V. R. Saunders, The periodic Hartree-Fock method and its implementation in the Crystal code. *Phys. Stat. Solidi (b)* **217**, 63–88 (2000).
12. E. Heifets, R. I. Eglitis, E. A. Kotomin, J. Maier, and G. Borstel, *Ab initio* modeling of surface structure for $SrTiO_3$ perovskite crystals. *Phys. Rev. B* **64**, 235417(5) (2001).
13. S. Piskunov, E. Heifets, R. I. Eglitis, and G. Borstel, Bulk properties and electronic structure of $SrTiO_3$, $BaTiO_3$, $PbTiO_3$ perovskites: an ab initio HF/DFT study. *Comput. Mater. Sci.* **29**, 165–178 (2004).
14. J. Paier, R. Hirschl, M. Marsman, and G. Kresse, The Perdew–Burke–Ernzerhof exchange-correlation functional applied to the G2-1 test set using a plane-wave basis set. *J. Chem. Phys.* **122**, 234102(13) (2005).
15. V. R. Saunders, R. Dovesi, C. Roetti, R. Orlando, C. M. Zicovich-Wilson, N. M. Harrison, K. Doll, B. Civalleri, I. J. Bush, Ph. D'Arco, and M. Llunell, CRYSTAL-03 User Manual (University of Turin, 2003).
16. A. D. Becke, Density-functional thermochemistry. III. The role of exact exchange. *J. Chem. Phys.* **98**, 5648(7) (1993).
17. P. J. Hay and W. R. Wadt, Ab initio effective core potentials for molecular calculations. Potentials for the transition metal atoms Sc to Hg. *J. Chem. Phys.* **82**, 270–283 (1984).
18. S. Piskunov, A. Gopeyenko, E. A. Kotomin, Yu. F. Zhukovskii, and D. E. Ellis, Atomic and electronic structure of perfect and defective $PbZrO_3$ perovskite: Hybrid DFT calculations of cubic and orthorhombic phases. *Comput. Mater. Sci.* **41**, 195–201 (2007).
19. J. Carrasco, F. Illas, N. Lopez, E. A. Kotomin, Yu. F. Zhukovskii, R. A. Evarestov, Yu. A. Mastrikov, S. Piskunov, and J. Maier, First-principles calculations of the atomic and electronic

structure of *F* centers in the bulk and on the (001) surface of $SrTiO_3$. *Phys. Rev. B* **73**, 064106(11) (2006).
20. H. J. Monkhorst and J. D. Pack, Special points for Brillouin-zone integrations. *Phys. Rev. B* **13**, 5188–5192 (1976).
21. G. Gilat, General analytic method of zone integration for joint densities of states in metals. *Phys. Rev. B* **26**, 2243–2246 (1982).
22. G. Kresse and J. Hafner, VASP Guide (University of Vienna, 2003).
23. S. Piskunov, E. Heifets, E. A. Kotomin, J. Maier, R. I. Eglitis, and G. Borstel, Hybrid DFT calculations of the atomic and electronic structure for ABO_3 perovskite (001) surfaces. *Surf. Sci.* **575**, 75–88 (2005).
24. E. A. Kotomin, S. Piskunov, Yu. F. Zhukovskii, R. I. Eglitis, A. Gopejenko, and D. E. Ellis, The electronic properties of an oxygen vacancy at ZrO_2-terminated (001) surfaces of cubic $PbZrO_3$: Computer simulations from the first principles. *Phys. Chem. Chem. Phys*. 10:4258–4263 (2008).